Radial electron fluence around ion tracks as a new physical parameter for the detection threshold of PADC using Geant4-DNA toolkit

Kusumoto, Tamon ; Bitar, Ziad EL ; Okada, Shogo ; Gillet, Pierre ; Arbor, Nicolas ; Kanasaki, Masato ; Mori, Yutaka ; Oda, Keiji ;…

(Citation)
Radiation Measurements,118:50-53

(Issue Date)
2018-11

(Resource Type)
journal article

(Version)
Accepted Manuscript

(URL)
https://hdl.handle.net/20.500.14094/90005202

Radial electron fluence around ion tracks as a new physical parameter for the detection threshold of PADC using Geant4-DNA toolkit

Tamon Kusumoto[a,b,f], Ziad EL Bitar[b], Shogo Okada[c], Pierre Gillet[b], Nicolas Arbor[b], Masato Kanasaki[a], Yutaka Mori[a], Keiji Oda[a], Abdel-Mjid Nourreddine[b], Hisaya Kurashige[c], Michel Fromm[d], Pierre Cloutier[e], Andrew D Bass[e], Léon Sanche[e], Satoshi Kodaira[f], Rémi Barillon[b], and Tomoya Yamauchi[a]*

[a]*Graduate School of Maritime Sciences, Kobe University, 5-1-1 Fukaeminami-machi, Higashinada-ku, 658-0022 Kobe Japan*

[b]*Institut Pluridisciplinaire Hubert Curien (IPHC), Université de Strasbourg 23 rue du Loess, 67037 Strasbourg Cedex, France*

[c]*Organization for Advanced and Integrated Research, Kobe University, 1-1 Rokkodai, Nada-ku, 657-8501 Kobe Japan*

[d]*Université de Bourgogne-France-Comté, 16 Route de Gray, F-2530 Besançon Cedex, France*

[e]*Faculté de Medicine, Université de Sherbrooke, Sherbrooke, Canada J1H 5N4*

[f] *Radiation Measurement Research Team, National Institute of Radiological Sciences, National Institutes for Quantum and Radiological Science and Technology, 4-9-1 Anagawa, Inage-ku, 263-8555 Chiba, Japan*

The detection threshold of poly(allyl dyglycol carbonate), PADC, for C ions is determined as 55 eV/nm in stopping power, which is significantly higher than that for proton and He ions. The stopping power is not a universal parameter for expressing the detection threshold of PADC. A new physical parameter of Radial Electron Fluence around Ion Tracks, *REFIT*, is proposed to describe the detection threshold of PADC. It is defined as the number density of electrons passing through the surface of a cylinder of a certain radius that is co-axial with the trajectory. Furthermore, preliminary calculations are presently being performed using the Monte Carlo simulation code of Geant4-DNA. The values of the *REFIT* at the detection thresholds for each ion are of the same order. Several issues affecting implementation of the *REFIT* paramter are discussed. These include the effects of impact parameter relating to the initial locations of secondary electrons, the effects of electron attachment below the cut off energy of 7.4 eV and the necessity of a more physically realistic medium than water for Monte Carlo simultaions.

Keyword : Geant4-DNA, PADC, detection threshold, latent track, REFIT

*Corresponding author

e-mail: yamauchi@maritime.kobe-u.ac..jp (Tomoya Yamauchi)

1. Introduction

Poly allyl(diglycol carbonate), PADC, has been considered the most sensitive etched track detector and is widely known by the trade name of CR-39 (Cartwright et., 1978). When it is irradiated with protons or heavy ions, permanent damage in the form of latent tracks are generated along each ion path. After chemical etching, latent tracks are, above the detection threshold, observable with optical microscopes as etch pits (Somogyi et al., 1976). The track registration sensitivity, S, is defined as $S=V-1$, where V is the ratio of track etching velocity V_t to the bulk etching velocity V_b ($V \equiv V_t/V_b$). Assuming normal incidence and that V_t is constant with the etching depth, S has been derived as follows:

$$S = \frac{1+(r/G)^2}{1-(r/G)^2} - 1, \quad (1)$$

where r is the etch pit radius (in μm) and G is the thickness layer removed (in μm). Fig. 1 shows a repeat unit of PADC which is composed of a radio-sensitive and radio-torelant sections. The radio-sensitive secition comprises an ether and carbonate esters connected by ethylene groups. The radio-torelant part is the "polyethylene-like" network formed during the polymerization. The length of a repeat unit of PADC is about 2 nm. We have conducted a series of FT-IR spectrometric studies to understand the latent track structure of protons and heavy ions in PADC (Yamauchi, 2003; Mori et al., 2011; Kusumoto et al, 2016a). We demonstrated that at least two electrons are necessary to break the carbonate ester. Additionally, more than two radio-sensitive parts must be lost in track's radial direction, for the latent track be etchable (Kusumoto et al., 2016b). These results indicated that the number of electrons which pass through each single repeat unit is the critical factor in elucidating the difference between etchable tracks and un-etchable ones. In this study, we simulate the 3-D spatial distribution of secondary electrons around tracks of protons, He and C ions in the virtual PADC and obtain the number density of electrons as a function of the radial distance from the ion trajectory using the Geant4-DNA toolkit.

2. Simulation code and Experiments

A Monte Carlo simulation in the Geant4-DNA toolkit was performed to investigate the number of secondary electrons around ion tracks (Allison et al., 2003&2016; Agostinelli et al., 2003). We used the "G4EmDNAPhysics" physics constructor installed in Geant4-DNA ver. 10.3.p01, in which the discrete processes including ionization, electronic excitation, vibrational excitation, elastic scattering and

molecular attachment for electron was taken into account, for energies down to 7.4 eV. Furthermore, the ionization processes of heavy ions up to Fe^{26+} can be included (Incerti et al., 2014). In this study, rather than PADC, the target is set as a virtual stopping medium having the same chemical composition as water but a density of 1.31 g/cm^3, which is equivalent to that of PADC.

Commercially obtained PADC sheets of BARYOTRAK with a nominal thickness of 0.9 mm (Fukuvi Chemical Industry Co., Ltd., Japan), which were made from purified monomers were used to determine the detection threshold for etch pit formation. The PADC sheets were made as the stack during exposures to C ions with an incident energy of 135 MeV/u in ambient air at the biological irradiation room of the Heavy Ion Medical Accelerator, HIMAC, Chiba equipped in National Institute of Radiological Sciences, NIRS, in Japan. C ions were completely stopped within the PADC stack. We conducted etching tests for 4 hours in 6 M KOH solution kept at 70□ after the irradiations. The size of etch pit openings was measured by optical microscope (BX60-F3, OLYMPUS, Japan) operated by WinROOF ver. 5.04 imaging processor (MITANI Corporation, Japan).

3. Results and Discussion

3.1. Detection thresholds of PADC

Fig. 2(a) shows the track response of PADC to C ions as a function of the stopping power, as well as previously reported data for proton and He ion irradiations (Hassan et al., 2013). We have defined the detection threshold as the original point at which the evolution of etch pits starts along the latent track under the surface, when the chemical etching was progressing from the front surface each heavy ions entered (Yamauchi et al., 2017). In normal incidence, the threshold can be attained by extrapolating the fitted growth curves of each etch pit to zero radius. The thresholds are also expressed by the stopping power at the original points (Ziegler, 2004). The detection threshold for C ions is 55 eV/nm, which is greater than those of protons (17 eV/nm) and He ions (37 eV/nm) as indicated by arrows in Fig. 2(a). As shown in Fig. 2(a), the stopping power is not a universal parameter for expressing the sensitivity and the detection threshold. The Restricted Energy Loss, *REL*, in which the high energy components of secondary electrons has been assumed not to contribute to the track formation has been developed as a suitable parameter for track registration in polymeric detectors (Benton&Nix, 1969). For the cut-off energy, ω_0, of secondary electrons, a value of 200 eV has been used for PADC (Kodaira et al., 2013). The sensitivities of proton, He and C ions at each detection threshold are different from each other. This

suggests that it is impossible to describe the detection thresholds by a single value of *REL*. The radial dose distribution theory has also been used as a universal parameter for expressing the track etchability of LiF crystals irradiated with GeV ions (Shcwartz et al., 1998). This theory however could not simply applied to express the latent track structure in PADC (Barillon et al., 2015).

3.2. A New physical concept for the detection thresholds of PADC

In PADC, at least two electrons are required to break the carbonate ester (Kusumoto et al., 2016a) and more than two radio-sensitive parts must be lost in the track's radial direction for tracks to be etchable (Kusumoto et al, 2106b). Based on these experimental results, we focus on the most fundamental variable (i.e. number density of secondary electrons around ion trajectories) and propose the Radial Electron Fluence around Ion Tracks, *REFIT*, as a new physical parameter to express the detection threshold of PADC. *REFIT* is defined as the number density of secondary electrons that traverse a cylindrical surface co-axial with the ion trajectory. In general, fluence is defined as the number of particles incident on a sphere divided by the cross-sectional area of the sphere. In the present case, we count the electrons passing through the surface of a cylinder of a certain radius, because spatially, the tracks of secondary electrons are of cylindrical symmetry around the ion path. The inset sketch in Fig. 3 shows a simulation result for the electron tracks produced by C ions with an incident energy of 51 MeV/u whose trajectory is illustrated by the blue line. The secondary electron tracks are indicated as the red lines. The yellow points show the interaction points. The secondary electrons are assumed to originate from each point on the ion trajectory. The secondary electrons produce many further electrons before terminating their trajectory at some radius and individual history which depend on the initial energy of electrons. These further electrons are also calculated. We set-up a series of cylinders, with radius increasing in steps of 0.1 nm, and evaluated the number of electrons that crossed the sides of each cylinder in the both directions, forwards and backs. Fig. 3 indicates the *REFIT* for proton, He and C ions, which are calculated at the detection thresholds for each ion, as a function of the distance from ion's path. The values of *REFIT* decrease with increasing radius, and heavier ions have larger values. Unfortunately, we do not find a common value of *REFIT* at any radius. However, the values of *REFIT* at a radius of 1 nm, which is the half of the length of a repeat unit of PADC, are in agreement with a Multi-hit model that was experimentally obtained using low linear energy transfer, "*LET*", radiations, which indicates that at least two electrons are necessary to break the carbonate ester in PADC (Kusumoto et al., 2016a). Fig. 2 (b) represents the track response data as a function of the *REFIT* at a radius of 1 nm. The

arrows in the graph show the detection thresholds for each ion. Compared to the response curves in Fig.2 (a), those in Fig. 2 (b) are closer together. From this, we judge that the *REFIT* is an improved physical parameter relative to the stopping power.

3.3. Future issues of the new physical concept

To improve the accuracy of the simulation of the *REFIT*, we should address the following issues:

(I) In the present simulation, all secondary electrons are ejected from the ion trajectory. However, in reality, the primary ionization could occur at atoms distant from the trajectory. Fig. 4 shows the impact parameter, b ($b_{min} \leqq b \leqq b_{max}$), for ionization, which is the perpendicular distance at which the Coulomb force is likely to act to excite/ionize an atom (Durrani&Bull, 1987). The values of b_{min} and b_{max} at the detection thresholds for each ion are also indicated. In the case of C ions, even electrons at 5.4 nm from the track center are affected. This implies that when the impact parameter is considered in the simulation, the value of *REFIT* around track center will be lower than in the present case.

(II) The electrons with energies less than 7.4 eV, which is the cut-off energy in the simulations, can also act to cleave the chemical bonds by processes such as dissociative electron attachment, and could cause breaks in PADC (Bazin et al., 2009; Böhler et al., 2013; Alizadeh et al., 2016; Yildirim et al., 2010). We should thus consider the interactions of such low energy electrons in order to more accurately determine secondary electron histories and the density of such electrons around the ion's trajectory. Then, number of interactions of secondary electrons with medium should also be evaluated as another parameter, which can be treated as a universal one, and be compared to present model (Kai et al., 2018).

(III) A more physically realistic model for PADC should be used as the target instead of the virtual stopping media. Repeating the calculation in the materials that contain carbon atoms is a mandatory next step to improve the *REFIT*. The application of the Geant4-DNA to the DNA bases has been started (Francis et al., 2017) but further extensions of this model are required.

4. Conclusion

In this study, we determined the detection threshold of PADC for C ions as the stopping power of 55 eV/nm. The obtained value was greater than that for protons and He ions. We proposed the *REFIT* as a new alternative physical parameter to replace the stopping power and the *REL* for describing the detection threshold of PADC. The

values of *REFIT* at a radius of 1 nm were concordant with the experimentally obtained Multi-hits model for low *LET* radiations. In order to improve the accuracy of the values of the *REFIT* as a possible universal parameter for the detection threshold of PADC, three issues, must in the future be considered. These include the impact parameter, which is the perpendicular distance between the ion path and the initial locations of secondary electrons; the effects of low energy electron attachment below the present cut-off energy of 7.4 eV and the nature of virtual stopping medium in the Geant4-DNA. When these issues are solved, a door of the *REFIT* as a better scaling parameter, may be opened.

Acknowledgments

The authors express our thanks to the staff of NIRS-HIMAC for their support during the experiments. This study was made as a part of the Research Project with Heavy Ions at NIRS-HIMAC. This work was supported by JSPS KAKENHI Grant Number 16K05002.

References

Agostinelli, S., Allison, J., Amako, K., Apostolakis, J., Araujo, H., Arce, P., Asai, M., Axen, D., Banerjee, S., Barrand, G., Behner, F., Bellagamba, L., Boudreau, J., Broglia, L., Brunengo, A., Burkhardt, H., Chauvie, S., Chuma, J., Chytracek, R., Cooperman, G., Cosmo, G., Degtyarenko, P., Dell'Acqua, A., Depaola, G., Dietrich, D., Enami, R., Feliciello, A., Ferguson, C., Fesefeldt, H., Folger, G., Foppiano, F., Forti, A., Garelli, S., Giani, S., Giannitrapani, R., Gibin, G., Gómez Cadenas, G.G., González, I., Gracia Abril, G., Greeniaus, G., Greiner, W., Grichine, V., Grossheim, A., Guatelli, S., Gumplinger, P., Hamatsu, R., Hashimoto, K., Hasui, H., Heikkinen, A., Howard, A., Ivanchenko, V., Johnson, A., Jones, F.W., Kallenbach, J., Kanaya, N., Kawabata, M., Kawabata, Y., Kawaguti, M., Kelner, S., Kent, P., Kimura, A., Kodama, T., Kokoulin, R., Kossov, M., Kurashige, H., Lamanna, E., Lampén, T., Lara, V., Lefebure, V., Lei, F., Liendl, M., Lockman, W., Longo, F., Magni, S., Maire, M., Medernach, E., Minamimoto, K., Mora de Freitas, P., Morita, Y., Murakami, K., Nagamatu, M., Nartallo, R., Nieminen, P., Nishimura, T., Ohtsubo, K., Okamura, M., O'Neale, S., Oohata, Y., Paech, K., Perl, J., Pfeiffer, A., Pia, M.G., Ranjard, F., Rybin, A., Sadilov, S., Di Salvo, E., Santin, G., Sasaki, T., Savvas, N., Sawada, Y., Scherer, S., Sei, S., Sirotenko, V., Smith, D., Starkov, N., Soecker, H., Sulkimo, J., Takahata, M., Tanaka, S., Tcherniaev, E., Safai Tehrani, E., Tropeano, M., Truscott, P., Uno, H., Urban, L., Urban, P., Verderi, M., Walkden, A., Wander, W., Weber, H., Wellisch, J.P., Wenaus,

T., Williams, D.C., Wright, D., Yamada, T., Yoshida, J., Zschieche, D., 2003, GEANT4 - A simulation toolkit, *Nucl. Instrum. Meth. A* **506**, 250-303.

Alizadeh, E., Ptasińska, S., Sanche, L., 2016. Transient Anions in Radiobiology and Radiotherapy: From Gaseous Biomolecules to Condensed Organic and Biomolecular Solid, *Radiation Effects in Materials*, 179-230.

Allison, J., Amako, K., Apostolakis, J., Araujo, H., Arce Dubois, P., Asai, M., Barrand, G., Capra, R., Chauvie, S., Chytracek, R., Cirrone, G.A.P., Cooperman, G., Cosmo, G., Cuttone, G., Daquino, G.G., Donszelmann, M., Dressel, M., Folger, G., Foppiano, F., Generowicz, J., Grichine, V., Guatelli, S., Gumplinger, P., Heikkinen,A., Hrivnacova, I., Howard, A., Incerti, S., Ivanchenko, V., Johonson, T., Jones, F., Koi, T., Kokoulin, R., Kossov, M., Kurashige, H., Lara, V., Larsson, S., Lei, F., Link, Longo, F., Maire, M., Mantero, A., Mascialino, B., McLaren, I., Mendez Lorenzo, P., Minamimoto, K., Murakami, K., Nieminen, P., Pandola, L., Parlati, S., Peralta, L., Perl, J., Pfeiffer, A., Pia, M.G., Ribon, A., Rodrigues, P., Russo, G., Sadilov, S., Santin, G., Sasaki, T., Smith, D., Starkov, N., Tanaka, S., Tcherniaev, E., Tome, B., Trindade, A., Truscott, P., Urban, L., Verderi, M ., Walkden, A., Wellisch, J.P., Williams, D.C., Wright, D., Yoshida, H., 2006. *IEEE Trans on Nuclear Science* **53**, 270-278.

Allison, J., Amako, K., Apostolakis, J., Arce, P., Asai, M., Aso, T., Bagli, E., Bagulya, A., Banerjee, S., Barrand, G., Beck, B.R., Bogdanov, A.G., Brandt, D., Brown, J.M.C., Burkhardt, H., Canal, Ph., Cano-Ott, D., Chauvie, S., Cho, K., Cirrone, G.A.P., Cooperman, G., Cortés-Giraldo, M., Cosmo, G., Cuttoe, G., Depaola, G., Desorgher, L., Dong, X., Dotti, A., Elvira, V.D., Folger, G., Francis, Z., Galoya, A., Garnier, L., Gayer, M., Genser, K.L., Grichine, V.M., Guatelli, S., Guèye, P., Gumplinger, P., Howard, A.S., Hřivnáčová, I., Hwang, S., Incerti, S., Ivanchenko, A., Ivanchenko, V.N., Jones, F.W., Jun, S.Y., Kaitaniemi, P., Karakatsanis, N., Karamitros, M., Kelsey, M., Kimura, A., Koi, T., Kurashige, H., Lechner, A., Lee, S.B., Longo, F., Maire, M., Mancusi, D., Mantero, A., Mendoza, E., Morgan, B., Murakami, K., Nikitina, T., Pandola, L., Paprocki, P., Perl, J., Petrović, I., Pia, M.G., Pokorski, W., Russo, G., Satin, G., Sasaki, T., Sawkey, D., Shin, J.I., Strakovsky, I.I., Taborda, A., Tanaka, S., Tomé, B., Toshito, T., Tran, H.N., Truscott, P.R., Urban, L., Uzhinsky, V., Verbeke, J.M., Verderi, M., Wendt, B.L., Wenzei, H., Wright, D.H., Yamashita, T., Yarba, J., Yoshida, H., 2016. Recent developments in Geant4, *Nucl. Instrum. Meth. B*. **28**, 49-52.

Barillon, R., Yamauchi, T., Mori, Y., Raffy, Q., 2015. A first attempt to simulate oxidization effects on latent track structure in PADC combining the radial dose theory and radio-oxidation kinetic model. *Radiat. Meas.* 83, 1-4.

Bazin, M. Ptasińska, S. Bass, A.D. Sanche, L., 2009. Electron induced dissociation in condensed-phase nitromethane I: desorption of ionic fragments, *Phys. Chem. Chem. Phys.* 11, 1610-1618.

Benton, E.V., Nix, W.D., 1969. The restricted energy loss criterion for registration of charged particle in plastics, *Nucl. Instr. Meth*. 67, 343-347.

Böhler, E., Warneke, J. Swiderek, P., 2013. Control of chemical reactions and synthesis by low-energy electrons, *Chem. Soc. Rev*. 42, 9219.

Cartwright, B.G., Shirk, E.K., Price, P.B., 1978. A nuclear-track-recording polymer of unique sensitivity and resolution. *Nucl. Instrum. Meth. B*. 41, 447-460.

Durrani, S.A., Bull, R.K., 1987. Solid state nuclear track detection, *International series in natural philosophy* 111, p. 15-19.

Francis, Z., EL Bitar, Z., Incerti, S., Bernal, M.A., Karamitros, M., Tran, H.N. 2017. Calculation of lineal energies for water and DNA bases using the Rudd model cross sections integrated within the Geant4-DNA processes, *J. Appl. Phys*. 122, 014701.

Hassan, N.M., Matai, Y., Kusumoto, T., Mori, Y., Kanasaki, M., Oda, K., Kitamura, H., Konishi, K., Kodaira, S., Yasuda, N., Yamauchi, T., 2013. On the mechanism of the sensitization of PADC (Poly(allyl diglycol carbonate)) track detectors by carbon dioxide treatment. *Radiat. Meas.*, 59, 23-29.

Incerti, S., Psaltaki, M., Gillet, P., Barberet, Ph., Bardiés, M., Bernal, M.A., Bordage, M.-C., Breton, V., Davidkova, M., Delage, E., EL Bitar, Z., Francis, Z., Guatelli, S., Ivanchenko, A., Ivanchenko, V., Karamitros, M., Lee, S.B., Maigne, L., Meylan, S., Murakami, K., Nieminen, P., Payno, H., Perrot, Y., Petrovic, I., Pham, Q.T., Ristic-Fira, A. Santin, G., Sasaki, T., Seznec, H., Shin, J.I., Stepan, V., Tran, H.N., Villagrasa, C., The Geant4-DNA Collaboration, 2014. Simulating radial dose of ion tracks in liquid water simulated with Geant4-DNA: A comparative study, *Nucl. Instrum. Meth. B*. 333, 92-98.

Kai, T., Yokoya, A., Ukai, M., Fujii, K., Toigawa, T., Watanabe, R., 2018. A significant role of non-thermal equilibrated electrons in the formation of deleterious complex DNA damage, *Phys. Chem. Chem. Phys*. 20, 2838-2844.

Kodaira, S., Yasuda, N., Konishi, T., Kitamura, H., Kurano, M., Kawashima, Uchihori, H., Ogura, K., Benton, E.R. 2013. Caribration of CR-39 with atomic force microscope for the measurement of short range tracks from proton-induced target fragmentation reactions, *Radiat. Meas.* 50, 232-236.

Kusumoto, T., Mori, Y., Kanasaki, M., Oda, K., Kodaira, S., Honda, Y., Tojo, S., Barillon, R., Yamauchi, T., 2016a. Sudden increase of the radiation chemical yield for loss of carbonate ester in PADC detector where the track overlapping of 28 MeV electrons becomes significant. *JPS. Conf. Proc*. 11, 010001.

Kusumoto, T., Mori, Y., Kanasaki, M., Ikenaga, R., Oda, K., Kodaira, S., Kitamura, H., Barillon, R., Yamauchi, T., 2016b. Radiation chemical yields for the losses of typical functional groups in PADC films for high energy protons registered as unetchable tracks. *Radiat. Meas*. 87, 35-42.

Mori, Y., Yamauchi, T., Kanasaki, M., Maeda, Y., Oda, K., Kodaira, S., Konishi, T., Yasuda, N., Barillon, R., 2011. Radiation chemical yields for loss of ether and carbonate ester bonds in PADC films exposed to proton and heavy ion beams. *Radiat. Meas.* 46, 1147-1153.

Schwartz, K., Trautmann, C., Steckenreiter, T., Geib, O., Krämer, M., 1998. Damage and track morphology in LiF crystals irradiated with GeV ions. *Phys. Rev. B* 58, 11232.

Somogyi, G., Grabishe, K., Shcerzer, R., Enge, W., 1976. Revision of the concept of registration threshold in plastic track detectors. *Nucl. Instrum. Meth.* 109, 129-141.

Yamauchi, T., 2003. Studies on the nuclear tracks in CR-39 plastics. *Radiat. Meas.* 36, 73-81.

Yamauchi, T., Kusumoto, T., Mori, Y., Kanasaki, M., Oda, K., Kodaira, S., Barillon, R., 2017. Distinct step-like changes in G values for the losses of typical functional groups in poly(ethylene terephthalate) along B ion tracks around the detection threshold.

International Conference on Nuclear Tracks and Radiation Measurements, 28th August – 1st September, Strasbourg, France.

Yildirim, Y., Balcan, M., Bass, A.D., Cloutier, P., Sanche, L., 2010. Electron stimulated desorption of anions and cations from condensed allyl glycidyl ether, *Phys. Chem. Chem. Phys*. 12, 7950-7958.

Ziegler, J.F., 2004. SRIM-2003. *Nucl. Instrum. Meth. B*. 219-220, 1027-1036.

Figure Captions

Fig. 1. A repeat unit of PADC.

Fig. 2. Track response data as a function of the stopping power (a) and the *REFIT* at a radius of 1 nm (b). The arrows indicate the detection thresholds for each ion. The error bars indicate each standard deviation.

Fig. 3. The *REFIT* for proton, He and C ions. The values of *REFIT* are calculated at the detection thresholds for each ion. The inset sketch (color online) is a simulation results of the secondary electrons (red lines) from the C ion trajectory with an incident energy of 46 MeV/u (blue line). The yellow points show the interaction points.

Fig. 4. Impact parameter, b ($b_{min} \leqq b \leqq b_{max}$), for ionization against the energies of ions. The b is perpendicular distance at which the Coulomb force acts for excitation/ionization of an atom. The plotted points are concordant with the detection thresholds of PADC for each ion.

Fig. 1 Kusumoto et al., 2017

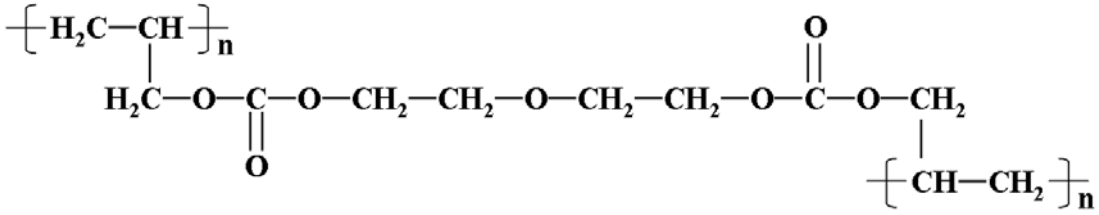

Fig. 2 Kusumoto et al., 2017

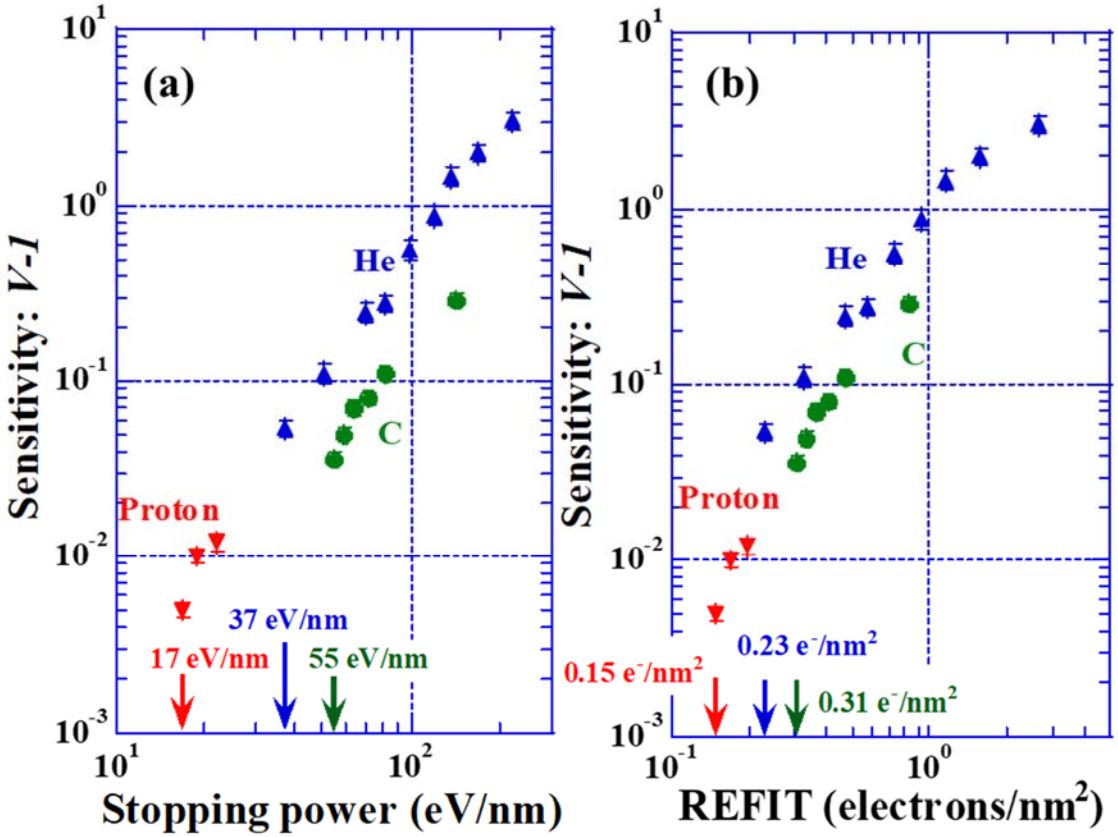

Fig. 3 Kusumoto et al., 2017

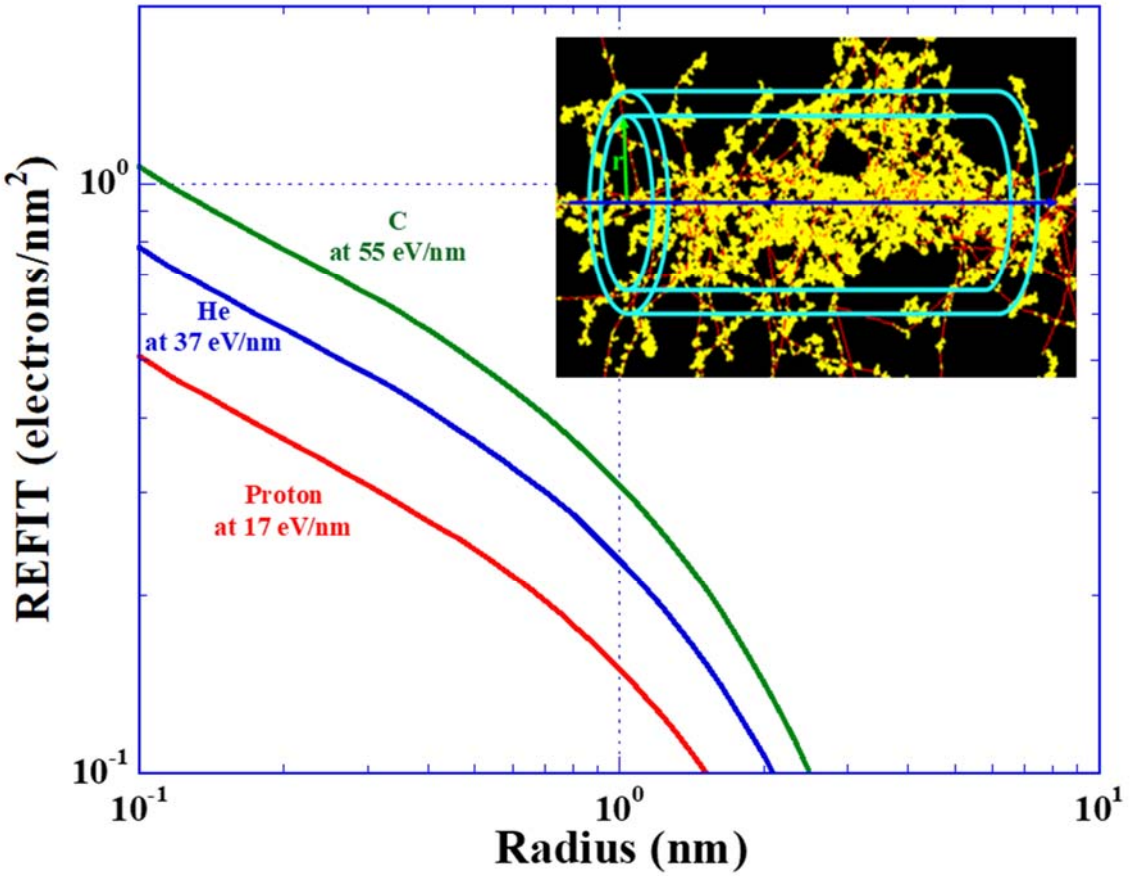

Fig. 4. Kusumoto et al., 2017